

# Bi-Layered Nanofibrous Mats For The Effective Treatment Of Infected Diabetic Wounds

Sunil Kumar Reddy Tamatam <sup>1</sup>, Srikanth Jupudi <sup>1\*</sup>, Teja Nayudu <sup>2</sup>, Manimaran Bhaskaran <sup>2</sup>, Veera Venkata Satyanarayana Reddy Karri <sup>2</sup>, Karri Ravikumar Reddy <sup>3</sup>.

<sup>1</sup>Department of Pharmaceutical Chemistry, JSS College of Pharmacy, JSS Academy of Higher Education & Research, Ooty, Nilgiris, Tamil Nadu, India.

<sup>2</sup>Department of Pharmaceutics, JSS College of Pharmacy, JSS Academy of Higher Education & Research, Ooty, Nilgiris, Tamil Nadu, India.

<sup>3</sup>Assistant professor, Department of EEE, Aditya university, Andhra Pradesh, India.

---

## Abstract:

*Diabetic foot ulcers (DFUs) remain one of the most severe complications of diabetes, often leading to chronic infections, prolonged hospitalization, and lower-limb amputations. Advanced wound dressings with multifunctional properties are essential to address both delayed tissue regeneration and infection control. In this study, a bi-layered electrospun nanofibrous mat was developed by combining two distinct functional layers: a PCL–Deferoxamine layer designed to promote angiogenesis and tissue regeneration, and a Chitosan–Collagen–PVA/Silver Sulfadiazine layer providing antibacterial protection and moisture balance. The mats were fabricated using optimized electrospinning parameters and characterized by SEM, FTIR, DSC, and XRD. SEM images revealed smooth, bead-free fibers with uniform morphology, while FTIR confirmed successful drug incorporation without significant chemical incompatibility. DSC and XRD results indicated a reduction in drug crystallinity, suggesting amorphous encapsulation, which is beneficial for solubility and sustained release. Collectively, the bilayer nanofibrous mats demonstrated favorable morphology, stability, and dual therapeutic potential, making them a promising candidate for the effective management of infected diabetic wounds.*

**Keywords:** Bi-layered nanofibers; Electrospinning; Deferoxamine; Silver sulfadiazine; Diabetic wound healing; Antibacterial wound dressing.

---

## INTRODUCTION:

Diabetes patients who have diabetic foot ulcers (DFU) are more likely to be hospitalized, suffer from morbidity, and die from the condition. DFU, one of the top 10 medical problems in the world, costs the healthcare system money (1). Over 90% of DFU cases, or one million amputations annually, have made it the primary cause of non-traumatic lower extremity amputations in the diabetic community. In a healthy individual, tissue regeneration occurs as a result of a well-regulated wound-healing process that includes the overlapping phases of hemostasis, inflammation, proliferation, and remodeling and lasts for a few weeks. Despite the fact that skin has the capacity for self-regeneration, chronic wounds like DFU are difficult to heal because of a variety of reasons, including a lack of oxygen, infection, and venous insufficiency(2).

Wound dressing materials made of exudate-absorbing polyurethane foam are employed in the present time (3). Recently, drug reservoirs made of electrospinning nanofibrous mats have been used due to their distinctive qualities, such as their high surface-to-volume ratios and simple construction. Here, we discuss numerous techniques for creating nanofibrous meshes that can be electrospinning and are drug- and gene-encapsulated. Numerous factors, such as the viscosity and ejection velocity of the polymeric solutions and the electrical voltage supplied to the system, influence the electrospinning process of producing nanofibrous mats. In order to prepare electrospinning nanofibers encasing drugs and genes, both single-nozzle and dual-nozzle systems are frequently used. These fibers are typically incorporated into the electrospinning mats either by physical mixing with polymeric solutions prior to electrospinning or by physical incorporation following electrospinning (4). The nanofiber's distinctive structural characteristics offer a favorable environment for promoting wound healing (5). Applications for electrospinning include

the filtering of subatomic particles, tissue engineering, dressings for wounds, medicine administration, artificial organs, and vascular grafts(6).

A well-known and widely used topical medication in wound care and management is silver sulfadiazine (SSD). It combines the antibacterial power of sulfadiazine with the antimicrobial characteristics of silver. SSD is highly effective against a wide variety of bacteria, including both gram-positive and gram-negative types, by releasing silver ions that prevent bacterial development and proliferation (7). The disruption of bacterial cell membranes, interference with cellular respiration, and hindrance of DNA replication caused by the silver ions ultimately results in the death of the bacteria. By fostering a moist environment that is ideal for wound healing and tissue regeneration, SSD plays a vital role in wound healing in addition to its powerful antibacterial action. It helps to lower inflammation, stop infections, and encourage the growth of granulation tissue(8).

Deferoxamine, traditionally known for its iron-chelating properties, is gaining attention for its potential as a wound healing and antimicrobial agent (9). Deferoxamine operates by binding and neutralizing excess free iron in the wound environment, which can be detrimental to wound healing due to its role in oxidative stress and inflammation. By reducing iron-mediated oxidative damage, deferoxamine helps to create a favorable wound healing environment. Additionally, deferoxamine possesses anti-inflammatory properties and has been shown to promote angiogenesis, collagen synthesis, and tissue regeneration. This multifaceted mechanism of action makes deferoxamine a promising candidate for enhancing wound healing and minimizing infection risk. Further research and clinical trials are essential to fully understand and optimize the application of deferoxamine in wound care for improved patient outcomes (9). Diabetic foot ulcers (DFUs) are among the most debilitating complications of diabetes, affecting nearly 15–25% of patients during their lifetime and accounting for up to 85% of diabetes-related lower-limb amputations worldwide (10). These chronic wounds are difficult to heal due to impaired angiogenesis, ischemia, neuropathy, and persistent infection. The increasing prevalence of multidrug-resistant microorganisms further complicates treatment outcomes and highlights the urgent need for advanced wound care strategies (11).

Conventional wound dressings such as gauze, hydrogels, and polyurethane foams primarily provide a physical barrier but lack bioactivity, often resulting in prolonged healing and frequent recurrence. In contrast, nanotechnology-based wound dressings offer multifunctional properties such as moisture balance, antimicrobial action, and bioactive molecule delivery, which are critical for chronic wound management (12).

Among these, electrospun nanofibers have gained considerable attention due to their ability to closely mimic the natural extracellular matrix (ECM), high surface-to-volume ratio for drug loading, and porous architecture that supports oxygen permeability and nutrient transport. Importantly, electrospinning enables the incorporation of multiple therapeutic agents, making it a versatile platform for designing advanced drug delivery systems in wound care (13).

Recent advances focus on bilayer or multilayer nanofibrous dressings, which integrate different functionalities in distinct layers. Such systems provide spatially controlled release, reduce drug–drug incompatibilities, and allow stage-specific wound healing support. For example, an outer antimicrobial layer can prevent infection, while an inner bioactive layer promotes angiogenesis and tissue regeneration (14). This dual-action approach has demonstrated superior wound closure rates and reduced infection recurrence in preclinical models, suggesting its strong potential for translation to clinical applications. Recent studies have demonstrated that incorporating therapeutic molecules into nanofibers can significantly enhance wound closure and tissue regeneration. For example, collagen–graphene oxide nanofibers loaded with deferoxamine (DFO) promoted angiogenesis and accelerated wound healing in diabetic rats (15), while PVA/chitosan/silk nanofibers co-loaded with DFO and ciprofloxacin provided both antibacterial activity and enhanced fibroblast migration in vitro (16). Mechanistically, DFO stabilizes HIF-1 $\alpha$ , upregulates VEGF, reduces reactive oxygen species (ROS), and enhances collagen deposition, thereby creating a favorable environment for regeneration (17). In parallel, silver sulfadiazine (SSD) continues to be a benchmark topical antimicrobial for infected wounds due to its broad-spectrum activity and ability to maintain a moist wound environment (18). Advances in electrospinning now allow

multilayer or core-shell systems that provide spatially and temporally controlled drug release, improving therapeutic precision and reducing drug-drug incompatibilities (19). Moreover, multilayer wound dressings, such as recently developed triple-layer electro spun nanofiber patches, have shown superior mechanical stability, sustained release, and faster wound closure in preclinical DFU models (20,21). Taken together, these findings highlight the potential of bilayer nanofibrous mats that integrate DFO for angiogenesis and SSD for infection control as a next-generation wound dressing system for diabetic wound management.

To reduce healing time and prevent infection throughout the wound healing process, the double-layered nanofibrous mat comprising Deferoxamine and Silver Sulfadiazine employed in this study might be regarded as an appropriate wound dressing.

## **MATERIALS AND METHODS:**

Polycaprolactone (PCL, 10% w/v) was dissolved in a chloroform-methanol mixture (8:2 v/v) and used as the base polymer for the preparation of the PCL-Deferoxamine nanofibers, with Deferoxamine incorporated at a concentration of 1% w/v. For the second solution, chitosan (200 mg) was dissolved in 20 mL of 1% acetic acid, while collagen (200 mg) was dispersed in 2 mL of distilled water; these were blended with 8 mL of polyvinyl alcohol (PVA, 20% w/v), and silver sulfadiazine was added at 1% w/v to obtain the drug-loaded polymeric solution. Electrospinning was performed using a standard setup comprising a high-voltage power supply, syringe pump, and a needle of defined diameter connected to a grounded collector plate. Additional laboratory materials such as syringes, aluminum foil, pipettes, gloves, and protective eyewear were used during the experimental procedures.

Optimization of the formulation was carried out by systematically varying both solution and electrospinning parameters to achieve uniform nanofiber morphology and reproducible characteristics. For solution parameters, different polymer concentrations (8%, 10%, and 12% w/v) were prepared to assess their influence on fiber formation, while drug concentrations were varied between 0.5%, 1%, and 1.5% w/v to study their effect on release kinetics and fiber integrity. The solvent system for PCL was optimized by testing chloroform-methanol ratios of 7:3, 8:2, and 9:1, and the viscosity of solutions was further adjusted by modifying either polymer concentration or solvent composition. Electrospinning parameters were then fine-tuned by applying voltages of 10, 15, and 20 kV to determine their impact on fiber morphology, with fiber diameter and bead formation examined using scanning electron microscopy (SEM). Flow rates of 0.4, 0.6, and 0.8 mL/h were tested to prevent needle clogging and improve fiber uniformity, while the distance between the needle tip and collector was varied at 6, 8, and 10 cm to regulate fiber deposition and solvent evaporation. Additionally, different needle gauges were employed to evaluate their effect on jet diameter and resulting fiber size.

### **PREPARATION OF SOLUTION A:**

**Step1: Preparation of polymeric solution A 1:** The electrospinning solution (Solution A 1) was prepared by dissolving PCL at a concentration of 10% (w/v) in a binary solvent system consisting of chloroform and methanol at a volume ratio of 8:2. The polymer solution was prepared by dissolving the calculated amount of PCL in the chloroform-methanol solvent mixture under continuous magnetic stirring at room temperature for 24 hours to ensure complete dissolution and homogenization of the polymer matrix.

**Step2: Preparation of drug polymeric solution A 2:** The electrospinning solution (Solution 2) was prepared by dissolving PCL at a concentration of 10% (w/v) in a binary solvent system consisting of chloroform and methanol at a volume ratio of 8:2. The polymer solution was prepared by first dissolving the calculated amount of PCL in the chloroform-methanol solvent mixture under continuous magnetic stirring at room temperature for 3 hours to ensure complete dissolution and homogenization. Subsequently, deferoxamine was incorporated into the polymer solution at 1% (w/w) relative to the polymer mass. The drug-loaded solution was stirred for an additional 1 hours at room temperature to achieve uniform drug distribution throughout the polymer matrix.

### **PREPARTON ELECTOSPING OF TOP LAYER POLYMERIC SOLUTION AND DRUG NANOFIBER SOLUTION A:**

**Step1: Preparation of NANOFIBER polymeric solution A 1:** The electrospinning parameters were set as follows: applied voltage of 15 kV, flow rate of 0.6  $\mu$  L / min, tip-to-collector distance of 8 cm, and a grounded aluminum foil-covered collector plate. The positive electrode was connected to the needle tip, while the collector served as the counter electrode. Electrospinning was performed for a duration of 6-8 hours to obtain sufficient fiber mat thickness for subsequent characterization.

**Step2: Preparation of NANOFIBER drug polymeric solution A 2:** The electrospinning parameters were set as follows: applied voltage of 15 kV, flow rate of 0.6  $\mu$  L / min, tip-to-collector distance of 8 cm, and a grounded aluminum foil-covered collector plate. The positive electrode was connected to the needle tip, while the collector served as the counter electrode. Electrospinning was performed for a duration of 6-8 hours to obtain sufficient fiber mat thickness for subsequent characterization.

#### **PREPARATION OF SOLUTION B:**

**Step1: Preparation of polymeric solution B 1:** The electrospinning solution (Solution B) was prepared by dissolving 200 mg of chitosan in 20 mL of 1% (v/v) acetic acid solution under continuous magnetic stirring until a clear solution was obtained. Separately, 200 mg of collagen was dispersed in 2 mL of distilled water with gentle stirring to ensure proper solubilization. In parallel, 20% (w/v) polyvinyl alcohol (PVA) was prepared, from which 8 mL was taken and mixed with the chitosan and collagen solutions. The resulting mixture was stirred magnetically at room temperature for 24 hours to obtain a homogeneous polymer blend suitable for electrospinning.

**Step2: Preparation of drug polymeric solution B 2:** The electrospinning solution (Solution B) was prepared by dissolving 200 mg of chitosan in 20 mL of 1% (v/v) acetic acid solution under continuous magnetic stirring at room temperature until a clear solution was obtained. Separately, 200 mg of collagen was dissolved in 2 mL of distilled water with gentle stirring. In parallel, 8 mL of 20% (w/v) polyvinyl alcohol (PVA) solution was prepared and added to the chitosan–collagen mixture. The polymer blend was stirred magnetically at room temperature for 3 hours to ensure complete dissolution and homogenization of the polymer matrix. Subsequently, silver sulphadiazine was incorporated into the solution at a concentration of 1% (w/v), followed by an additional 1 hour of stirring at room temperature to achieve uniform drug distribution throughout the nanofiber-forming solution.

#### **PREPARTON ELECTOSPING OF BOTTOM LAYER POLYMERIC SOLUTION AND DRUG NANOFIBER SOLUTION B:**

**Step1: Preparation of NANOFIBER polymeric solution B 1:** The electrospinning parameters were set as follows: an applied voltage of 28 kV, a flow rate of 0.4  $\mu$  L /min, and a tip-to-collector distance of 15 cm, with a grounded aluminum foil-covered collector plate serving as the deposition surface. The positive electrode was connected to the needle tip, while the collector functioned as the counter electrode. Electrospinning was carried out for 6–8 hours to obtain nanofiber mats with adequate thickness for subsequent characterization.

**Step2: Preparation of NANOFIBER drug polymeric solution B 2:** The electrospinning parameters were set as follows: an applied voltage of 28 kV, a flow rate of 0.4  $\mu$  L /min, and a tip-to-collector distance of 15 cm, with a grounded aluminum foil-covered collector plate serving as the deposition surface. The positive electrode was connected to the needle tip, while the collector functioned as the counter electrode. Electrospinning was carried out for 6–8 hours to obtain nanofiber mats with adequate thickness for subsequent characterization.

#### **Evaluation Parameters and Procedures:**

##### **SEM Analysis:**

The surface morphology and fiber diameter of the electrospun nanofibers were examined using scanning electron microscopy (SEM). Small sections of the nanofiber mats were carefully cut and mounted onto aluminum stubs with conductive carbon tape, followed by sputter-coating with a thin layer of gold or platinum to minimize charging effects. The prepared samples were then placed in the SEM chamber, and imaging was performed at an accelerating voltage in the range of 5–15 kV. Micrographs were captured at different magnifications to assess the overall fiber morphology, uniformity, and presence of bead formation, and fiber diameters were measured from the obtained images.

##### **FTIR Analysis:**

Fourier-transform infrared (FTIR) spectroscopy was performed to identify the functional groups present in the nanofibers and to confirm drug incorporation within the polymer matrix. A small quantity of nanofiber sample was finely ground and mixed with spectroscopic grade potassium bromide (KBr), followed by compression into a transparent pellet using a hydraulic press. The spectra were recorded in the wavelength range of 4000–400  $\text{cm}^{-1}$  using an FTIR spectrometer. The characteristic absorption peaks obtained were compared with standard reference spectra to verify the presence of specific functional groups and to assess possible drug–polymer interactions.

#### DSC Analysis:

Differential scanning calorimetry (DSC) was carried out to study the thermal behaviour of the nanofibers and to confirm drug incorporation within the polymeric matrix. Approximately 5–10 mg of sample was sealed in an aluminium pan and analysed using a DSC instrument under a nitrogen atmosphere to prevent oxidative degradation. The samples were heated at a constant rate (e.g., 10  $^{\circ}\text{C}/\text{min}$ ) over a suitable temperature range, and the resulting thermograms were recorded. The melting points, glass transition temperatures, and other thermal events were compared with those of pure polymers and drugs to evaluate possible drug–polymer interactions and changes in crystallinity.

#### XRD Analysis:

X-ray diffraction (XRD) was performed to investigate the crystalline or amorphous nature of the nanofibers and to assess structural changes after drug incorporation. The nanofiber samples were placed on a sample holder and scanned over a  $2\theta$  range of  $5^{\circ}$ – $60^{\circ}$  using Cu  $K\alpha$  radiation ( $\lambda = 1.5406 \text{ \AA}$ ) operated at 40 kV and 30 mA. The diffraction patterns obtained were analyzed to identify the presence of characteristic crystalline peaks of the polymers and drugs, and to evaluate whether the drug existed in a crystalline or amorphous form within the nanofiber matrix.

### RESULT AND DISCUSSION:

Table 1: Solubility characteristics of the solvents and polymers used in nanofiber preparation.

S. No	Solvent	Inference
1.	Distilled water	Universal solvent, dissolves hydrophilic compounds; insoluble for most hydrophobic polymers like PCL.
2.	Polycaprolactone (PCL)	Hydrophobic, insoluble in water; soluble in chloroform, dichloromethane, acetone, and some organic solvents.
3.	Chloroform	Good organic solvent; dissolves hydrophobic polymers like PCL but not hydrophilic ones like PVA, chitosan, or collagen.
4.	Methanol	Polar protic solvent; miscible with water; dissolves small polar molecules but not PCL; limited solubility for chitosan in acidic condition.
5.	Chitosan	Insoluble in water and organic solvents; soluble in dilute acidic aqueous solutions (e.g., acetic acid, HCl) due to protonation of amino groups.
6.	Collagen	Water-insoluble in native state; dispersible in acidic aqueous solutions; denatured collagen (gelatin) is water-soluble.
7.	Polyvinyl alcohol (PVA)	Hydrophilic, soluble in water; insoluble in organic solvents like chloroform; forms stable aqueous solutions.

#### SEM Imaging:

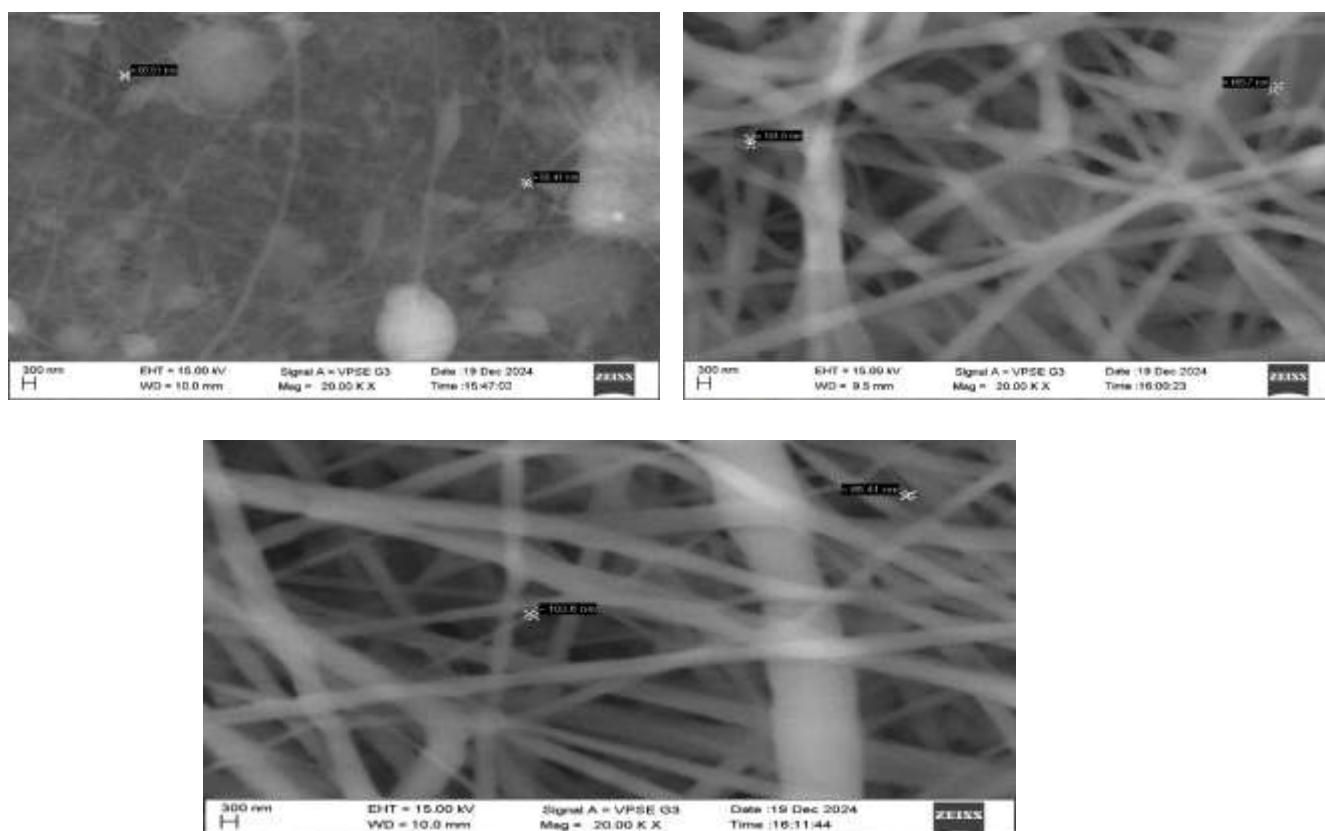
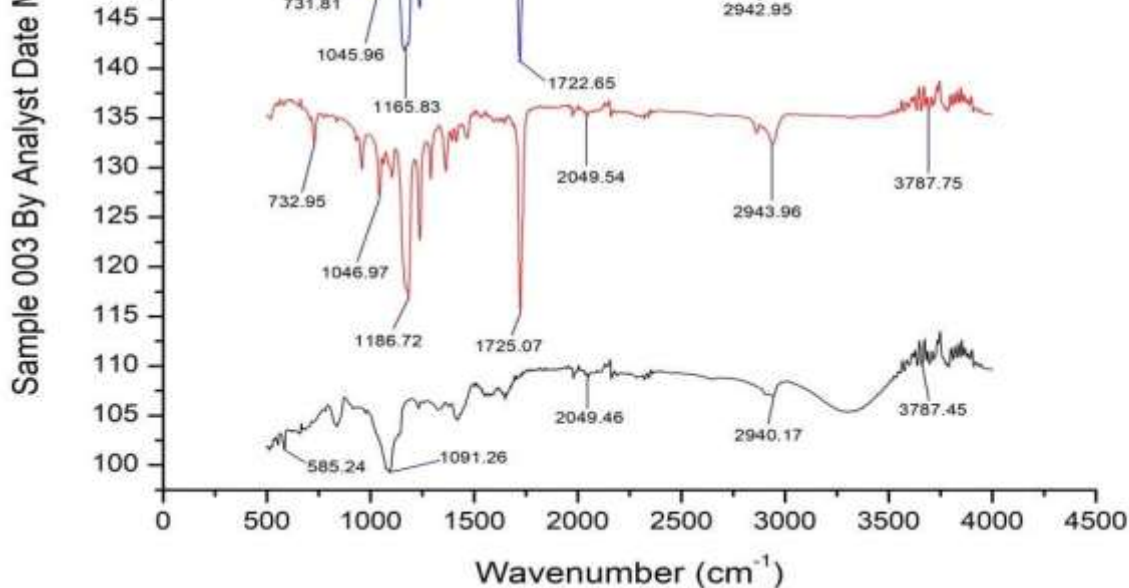


**Figure1: SEM image of nanofiber**

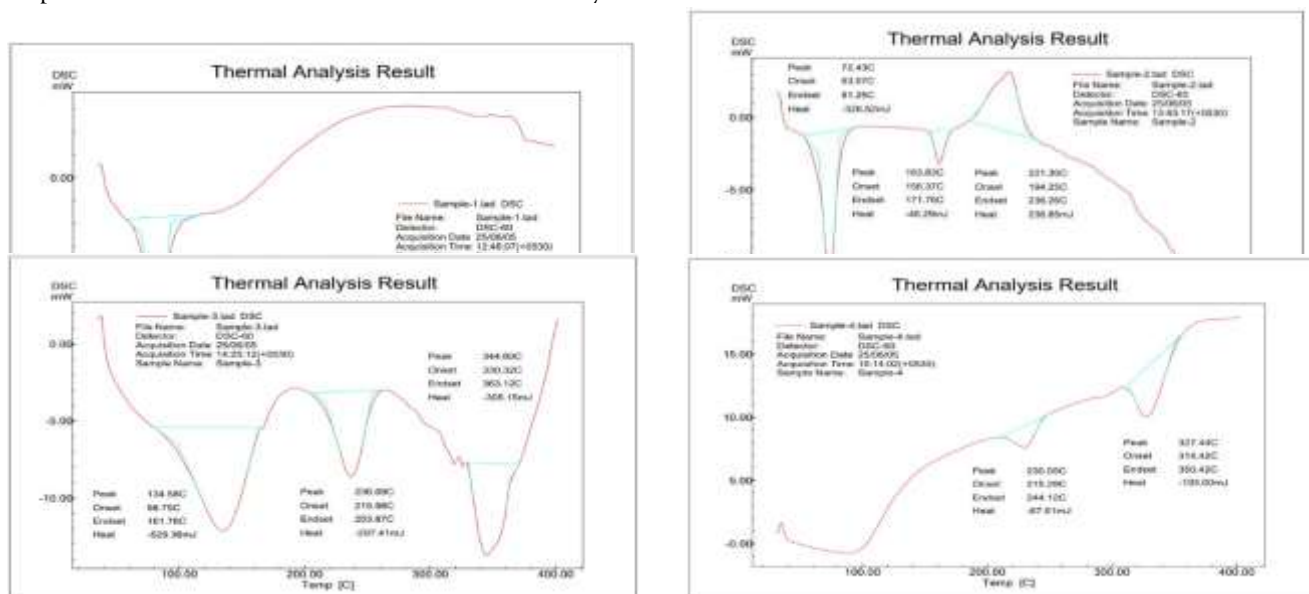
SEM micrographs revealed that the electro spun nanofibers exhibited a smooth, bead-free, and continuous morphology with uniform orientation. The PCL-deferoxamine nanofibers (top layer) showed consistent fibre thickness with an interconnected porous structure favourable for oxygen and nutrient transport, thus supporting wound healing. In contrast, the Chitosan–Collagen–PVA/SSD nanofibers (bottom layer) displayed a slightly rougher texture due to the incorporation of hydrophilic polymers and drug molecules, which contributed to enhanced drug encapsulation and release behaviour (Figure1). The average fibre diameters of both layers were within the nanometre to sub-micrometre range (100–800 nm), indicating successful optimization of electrospinning parameters. The interconnected porous network observed in the bilayer nanofibrous mat is advantageous for wound healing, as it facilitates exudate absorption, cell adhesion, and tissue regeneration. Additionally, the uniform morphology confirmed that the chosen polymer concentration, applied voltage, and flow rate were optimized for stable fibre formation without bead defects.

#### **FTIR Analysis:**

**Figure 2: FTIR Spectra of nanofibrous**



hydrogen bonding without significant chemical modification. Similarly, the Chitosan-Collagen-PVA/SSD nanofibers exhibited the characteristic peaks of both the polymer blend and SSD, with the presence of amide I and II peaks alongside S=O stretching vibrations confirming successful drug incorporation (Figure 2). FTIR analysis demonstrated that the characteristic peaks of both drugs and polymers were preserved with only minor shifts, suggesting effective drug loading and the absence of major chemical incompatibility, while hydrogen bonding interactions promoted stability and uniform dispersion within the nanofiber matrix. **DSC Analysis:**



(Deferoxamine)

Figure 6: (Silver Sulfadiazine):

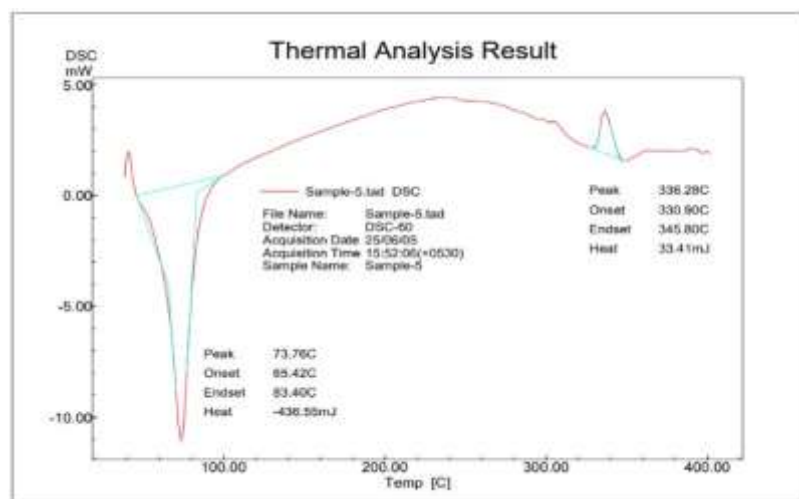


Figure 7: (Drug-loaded nanofibers)

DSC analysis revealed a sharp melting peak for PCL nanofibers at 59–62 °C, confirming their semicrystalline nature, while the Chitosan–Collagen–PVA nanofibers showed a broad endothermic band at 80–110 °C due to bound water loss and minor transitions at 220–250 °C from polymer degradation. Deferoxamine exhibited a broad endotherm at 150–160 °C, and Silver Sulfadiazine showed a sharp melting peak at 255–260 °C, confirming their crystalline properties. In drug-loaded nanofibers, drug peaks were diminished or broadened with polymer transitions retained, indicating successful encapsulation in an amorphous or dispersed state.

FTIR spectra of pure polymers, drugs, and drug-loaded nanofibrous mats were recorded in the range of 4000–400  $\text{cm}^{-1}$  to confirm functional groups and drug incorporation. The PCL spectrum displayed characteristic peaks at  $\sim 2945$  and  $\sim 2865$   $\text{cm}^{-1}$  corresponding to C–H asymmetric and symmetric stretching vibrations, a strong absorption band at  $\sim 1720$   $\text{cm}^{-1}$  due to ester carbonyl (C=O) stretching, and peaks at 1290–1160  $\text{cm}^{-1}$  representing C–O–C stretching (Figure 3). The Chitosan–Collagen–PVA blend showed a broad band between 3200–3400  $\text{cm}^{-1}$  attributable to O–H and N–H stretching, peaks at  $\sim 1630$  and  $\sim 1540$   $\text{cm}^{-1}$  corresponding to amide I and amide II of collagen, and a band at 1080–1150  $\text{cm}^{-1}$  assigned to C–O stretching of PVA (Figure 4). Deferoxamine exhibited a broad band near 3400  $\text{cm}^{-1}$  for –OH and –NH stretching along with amide vibrations at  $\sim 1650$  and 1540  $\text{cm}^{-1}$ , while Silver Sulfadiazine showed peaks at  $\sim 3320$   $\text{cm}^{-1}$  (N–H stretching),  $\sim 1650$   $\text{cm}^{-1}$  (C=O stretching), and 1150–1250  $\text{cm}^{-1}$  (S=O stretching) (Figure 5). In drug-loaded nanofibers, the PCL–Deferoxamine system retained the characteristic PCL peaks with slight shifts and broadening in the –OH/NH region, indicating drug encapsulation through hydrogen bonding without significant chemical modification. Similarly, the Chitosan–Collagen–PVA/SSD nanofibers exhibited the characteristic peaks of both the polymer blend and SSD, with the presence of amide I and II peaks alongside S=O stretching vibrations confirming successful drug incorporation (Figure 6). FTIR analysis demonstrated that the characteristic peaks of both drugs and polymers were preserved with only minor shifts, suggesting effective drug loading and the absence of major chemical incompatibility, while hydrogen bonding interactions promoted stability and uniform dispersion within the nanofiber matrix (Figure 7). **XRD Analysis:**

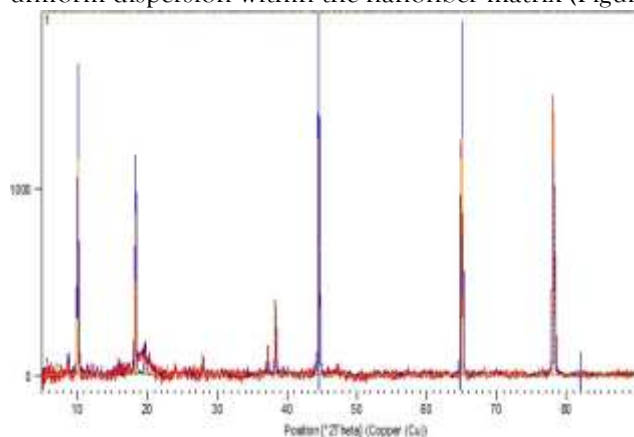


Figure8: (PCL nanofibers)

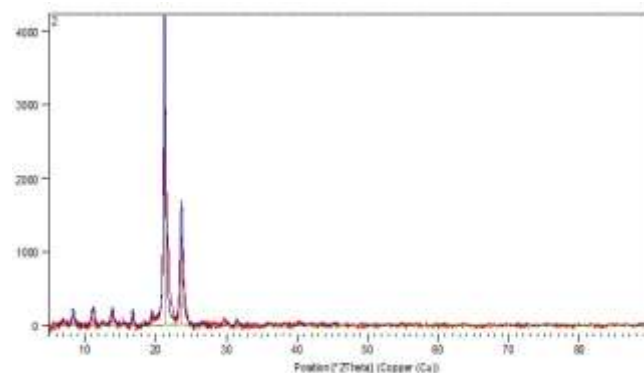
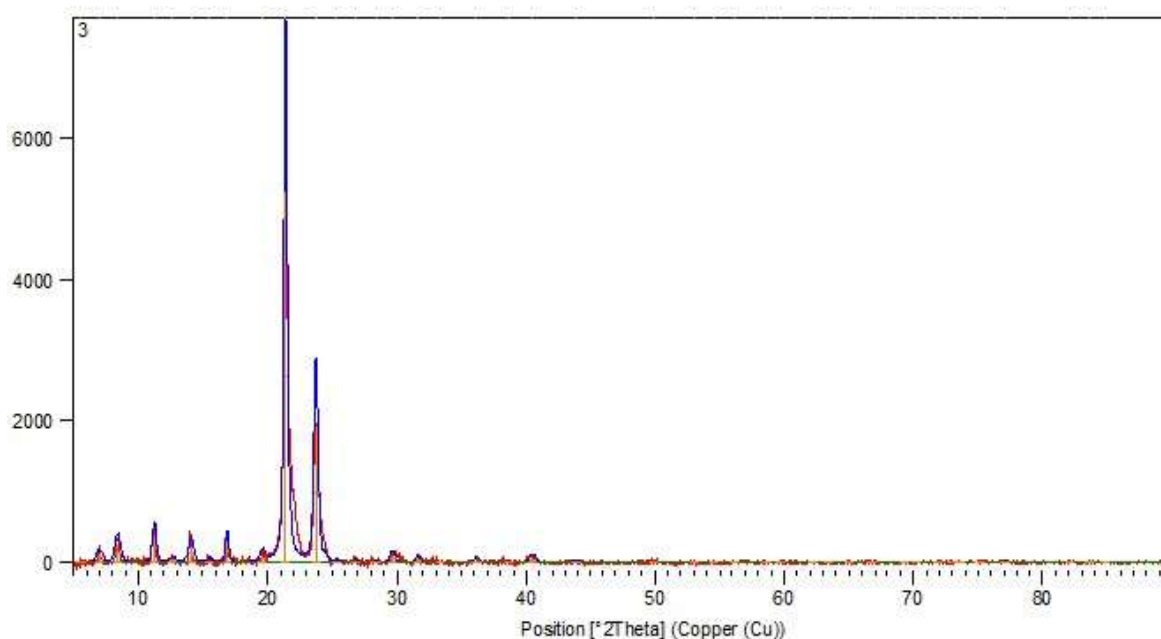


Figure9:Chitosan,Collagen,PVA





**Figure 10: (Drug-loaded nanofibers)**

The XRD diffractograms of pure polymers, drugs, and drug-loaded nanofibers were analyzed to assess their crystalline and amorphous characteristics. PCL displayed distinct diffraction peaks at  $2\theta \approx 21.5^\circ$  and  $23.8^\circ$ , confirming its semi-crystalline nature, whereas the Chitosan–Collagen–PVA blend exhibited a broad halo in the range of  $2\theta = 18\text{--}22^\circ$ , reflecting its predominantly amorphous structure with minor semi-crystallinity due to PVA (Figure 8). Deferoxamine showed sharp crystalline peaks between  $2\theta = 15\text{--}25^\circ$ , while Silver Sulfadiazine presented intense crystalline reflections between  $2\theta = 18\text{--}30^\circ$ , both confirming their crystalline nature (Figure 9). In drug-loaded nanofibers, the characteristic PCL peaks were retained with reduced intensity, and the crystalline peaks of Deferoxamine disappeared, suggesting its incorporation in an amorphous or molecularly dispersed form (Figure 10). Similarly, the amorphous halo of the Chitosan–Collagen–PVA blend was preserved, with a marked reduction in the crystalline peaks of SSD, indicating successful drug entrapment and decreased crystallinity. Overall, these findings demonstrate that electrospinning reduced the crystallinity of the drugs, enhancing their amorphous state, which is beneficial for improving solubility and supporting sustained drug release in wound healing applications.

## CONCLUSION:

A bi-layered electrospun nanofibrous mat incorporating Deferoxamine and Silver Sulfadiazine was successfully developed and characterized for the treatment of infected diabetic wounds. SEM analysis confirmed the formation of uniform, bead-free fibers with an interconnected porous structure favorable for oxygen exchange, nutrient diffusion, and exudate absorption. FTIR spectra verified successful drug incorporation without major chemical incompatibilities, while DSC and XRD analyses demonstrated that both drugs were present in a molecularly dispersed or amorphous form, enhancing solubility, stability, and controlled release. The bilayer configuration provided synergistic benefits, with the PCL–Deferoxamine layer supporting angiogenesis and tissue regeneration, and the Chitosan–Collagen–PVA/SSD layer delivering antimicrobial protection and moisture balance. These combined features highlight the potential of the fabricated nanofibrous mat as an effective wound dressing for diabetic foot ulcers. Future investigations involving in vitro release kinetics, antimicrobial assays, and in vivo wound healing studies are warranted to further establish its clinical applicability.

## REFERENCE:

1. Wang J, Windbergs M. Functional electrospun fibers for the treatment of human skin wounds. *Eur J Pharm Biopharm.* 2017 Oct 1;119:283–99.

2. Choudhury H, Pandey M, Lim YQ, Low CY, Lee CT, Marilyn TCL, et al. Silver nanoparticles: Advanced and promising technology in diabetic wound therapy. *Mater Sci Eng C*. 2020 Jul 1;112:110925.
3. Lakshman LR, Shalumon KT, Nair SV, Jayakumar R, Nair SV. Preparation of Silver Nanoparticles Incorporated Electrospun Polyurethane Nano-fibrous Mat for Wound Dressing. *J Macromol Sci Part A*. 2010 Aug 31;47(10):1012–8.
4. Choi JS, Kim HS, Yoo HS. Electrospinning strategies of drug-incorporated nanofibrous mats for wound recovery. *Drug Deliv Transl Res*. 2015 Apr 1;5(2):137–45.
5. Rho KS, Jeong L, Lee G, Seo BM, Park YJ, Hong SD, et al. Electrospinning of collagen nanofibers: Effects on the behavior of normal human keratinocytes and early-stage wound healing. *Biomaterials*. 2006 Mar 1;27(8):1452–61.
6. Yoo HS, Kim TG, Park TG. Surface-functionalized electrospun nanofibers for tissue engineering and drug delivery. *Adv Drug Deliv Rev*. 2009 Oct 5;61(12):1033–42.
7. Ostlie DJ, Juang D, Aguayo P, Pettiford-Cunningham JP, Erkmann EA, Rash DE, et al. Topical silver sulfadiazine vs collagenase ointment for the treatment of partial thickness burns in children: a prospective randomized trial. *J Pediatr Surg*. 2012 Jun 1;47(6):1204–7.
8. Khattak S, Qin XT, Huang LH, Xie YY, Jia SR, Zhong C. Preparation and characterization of antibacterial bacterial cellulose/chitosan hydrogels impregnated with silver sulfadiazine. *Int J Biol Macromol*. 2021 Oct 31;189:483–93.
9. Holden P, Nair LS. Deferoxamine: An Angiogenic and Antioxidant Molecule for Tissue Regeneration. *Tissue Eng Part B Rev*. 2019 Dec;25(6):461–70.
10. Armstrong DG, Boulton AJM, Bus SA. Diabetic foot ulcers and their recurrence. *N Engl J Med*. 2017;376(24):236775.
11. Zhang Y, Lazzarini PA, McPhail SM, van Netten JJ, Armstrong DG, Pacella RE. Global epidemiology of diabetic foot ulceration: a systematic review and meta-analysis. *Ann Med*. 2020;52(8):567–77.
12. Gupta A, Kedige SD, Jain K. Emerging therapies for diabetic foot ulcers: a systematic review. *J Diabetes Complications*. 2022;36(5):108176.
13. Ravindra S, Murahari M, Singh J, Prakash J, Rao S, Prabhu V, et al. Nanofiber-based drug delivery systems for skin regeneration and wound healing applications. *J Drug Deliv Sci Technol*. 2021;64:102617.
14. Jiang T, Carbone EJ, Lo KW-H, Laurencin CT. Electrospinning of polymer nanofibers for tissue regeneration. *Prog Polym Sci*. 2021;120:101876.
15. Shalumon KT, Anulekha KH, Nair SV, Chennazhi KP, Jayakumar R. Multilayer electrospun nanofibrous mats for wound healing applications. *J Mater Chem B*. 2019;7(27):4425–37.
16. Zhao Y, Chen J, Zhou M, Zhang G, Wu W, Wang Z, Sun J, Zhong A. Desferrioxamine-laden collagen-graphene oxide nanofiber scaffold promotes angiogenesis and diabetic wound healing in rats. *Int J Nanomedicine*. 2024;19:10551–68.
17. In vitro investigation of PVA/chitosan/silk electrospun mat loaded with deferoxamine and ciprofloxacin. *J Drug Deliv Sci Technol*. 2023.
18. Chelating the valley of death: Deferoxamine's path from bench to wound clinic. *Front Med*. 2023.
19. Nanofiber-based systems intended for diabetes. *J Nanobiotechnology*. 2021.
20. Enhancing diabetic wound healing: advances in electrospun scaffolds. *Front Bioeng Biotechnol*. 2024.
21. Artificial, triple-layered nanomembranous wound patch for DFU intervention. *Materials*. 2018.